Knee Surg Sports Traumatol Arthrosc
DOI 10.1007/s00167-014-3167-2

Post-cam mechanics and tibiofemoral kinematics: a dynamic in vitro analysis of eight posterior-stabilized total knee designs

N. Arnout · L. Vanlommel · J. Vanlommel · J. P. Luyckx · L. Labey · B. Innocenti · J. Victor · J. Bellemans

N. Arnout (*) · J. Victor Orthopedie en Traumatologie, University Hospital Ghent, De Pintelaan 185, 9000 Ghent, Belgium e-mail: nelearnout@yahoo.com

L. Vanlommel · J. Vanlommel · J. Bellemans University Hospitals Leuven, Weligerveld 1, 3012 Ghent, Belgium

J. P. Luyckx · L. Labey · B. Innocenti European Centre for Knee Research, Technologielaan, Heverlee, Belgium

L. Labey Department of Mechanical engineering, Biomechanics Section, Catholic University of Leuven, Louvain, Belgium

B. Innocenti BeAMS Department, École Polytechnique de Bruxelles, Université Libre de Bruxelles, Brussels, Belgium

J. Bellemans ZOL, Genk, Belgium

Abstract

Purpose

Posterior cruciate ligament (PCL)-substituting total knee arthroplasty (TKA) designs were introduced to avoid paradoxical roll forward of the femur and to optimize knee kinematics. The aim of this in vitro study was to investigate post-cam function and contact mechanics and relate it to knee kinematics during squatting in eight contemporary posterior-stabilized TKA designs.

Methods

All prostheses were fixed on custom-designed metal fixtures and mounted in a knee rig and five sequential- loaded squats were performed between 30° and 130° of flexion. Contact pressure and contact area were measured using pressure-sensitive Tekscan sensors on the posterior face of the post. Kinematics was recorded with reflective markers and infrared light-capturing cameras.

Results

The post-cam mechanisms analyzed in this study are very variable in terms of design features. This leads to large variations in terms of the flexion angle at which the post and cam engage maximal contact force, contact pressure and contact area. We found that more functional postcam mechanisms, which engage at lower flexion angle and have a similar behavior as normal PCL function, generally show more normal rollback and tibial rotation at the expense of higher contact forces and pressures. All designs show high contact forces. A positive correlation was found between contact force and initial contact angle.

Conclusion

Post-cam contact mechanics and kinematics were documented in a standardized setting. Post-cam contact mechanics are correlated with post-cam function. Outcomes of this study can help to develop more functional designs in future. nevertheless, a compromise will always be made between functional requirements and risk of failure. We assume that more normal knee kinematics leads to more patient satisfaction because of better mobility. Understanding of the post-cam mechanism, and knowing how this system really works, is maybe the clue in further development of new total knee designs.

Keywords

In vitro study · Posterior-stabilized TKA · Post-cam failure · Kinematics

Introduction

Posterior-stabilized total knee arthroplasty (PS TKA) designs were originally introduced in the seventies as an alternative for the existing cruciate-retaining (CR) designs. These CR implants often led to paradoxical motion with sliding forward of the femur on the tibia. This was (and is) believed to be partly due to incorrect balancing of the posterior cruciate ligament (PCL) in CR TKA, since the PCL is the main anteroposterior stabilizer, at least in the natural knee [7]. Correct balancing of the PCL proved to be one of the most challenging steps in TKA and even if a well-balanced PCL was achieved during surgery, the question remained whether this had a lasting effect in the long term. Oftentimes, loss of function of the PCL was noticed or suspected later on [31].

For these reasons, it seemed logical to replace the PCL rather than retaining it. Obviously, one needed a mechanism then to compensate for the loss of this important ligament. From an engineering point of view, the use of a post and cam mechanism was a straightforward choice. From all conceivable mechanisms, adding a post to the polyethylene insert and a cam to the femoral component is a relatively simple and at the same time functionally-robust solution. First of all, the number of design parameters is relatively limited. For a basic post-cam mechanism, seven design decisions suffice: post AP position, post size (height, width and depth), cam position (distance from the posterior edge and height above the joint line) and cam radius. Moreover, while design choices usually influence different aspects of function simultaneously, this is not so much the case in post and cam mechanisms. Indeed, post and cam positions are the parameters that mainly determine the function of the mechanism and are the primary variables (flexion angle at which the post and cam engage and the amount of femoral posterior motion which occurs thereafter), while post size and cam radius are the parameters that determine the strength, stiffness and stability of the mechanism. Real post and cam mechanisms deviate from this basic design layout of course, because other aspects need to be taken into account as well. Avoiding impingement with the patella anteriorly in flexion, subluxation of the knee, wear of the post are all concerns that need to be taken into account and will lead to deviations from the basic design layout [9].

With PS designs, kinematics was expected to be more natural although this is controversial and probably dependent on both implant design and surgical technique [3, 23]. Under 50° of flexion, the PCL is not functional [24]. PCL and post-cam mechanisms act in flexion. At low flexion angles, PCL deficient knees and CR and PS TKA designs show similar knee function. In flexion, PS designs

behave more normal than CR designs in terms of femoral posterior motion and have contact forces in the post-cam mechanism that are more similar to normal PCL forces. But still there is a difference compared with the native knee [13].

No clinical superiority of one type has been proven in the past, and overall survival for both types of prostheses is good [27].

However, adding constraint and contact surface always carries the risk of adding a new failure site. Post-cam failures are described such as breakage, dislocations and failure of guided motion [2, 8, 13, 16, 21]. Transmission of high stresses to the modular and bone–implant interfaces potentially leads to backside wear or loosening [5, 19, 20, 30]. Many designs of cam mechanisms are available, and different contact mechanics and tibiofemoral kinematics exist [11]. Design differences such as post-cam position and post and cam shape exist. There is a paucity of quantitative post-cam design description in the orthopedic literature. For this reason, an in vitro dynamic experiment was set up to analyze post and cam contact mechanics (force and pressure) in a set of contemporary PS knee implants and relate this to engagement angle and tibiofemoral kinematics.

Failure of the post-cam system can give raise to instability feeling and patient unsatisfaction [9, 32]. We assumed that more normal knee kinematics leads to more patient satisfaction because of better mobility. Understanding of the post-cam mechanism, and knowing how this system really works, is maybe the clue in further development of new total knee designs.

The objective of our study was threefold:

First, to document the contact force, pressure, distribution and location in currently available post-cam mechanisms in a standardized setting.

Second, to relate the differences in contact mechanics to differences in design features and kinematics.

Third, to compare kinematics of different post-cam mechanisms with the kinematics of a normal knee during a similar-loaded motor task.

Materials and methods

Test rig

The test setup is shown in Fig. 1. A dynamic knee kinematics simulator, based on the Oxford rig, was used in this study. It consists of a hip joint and an ankle joint, in which an upper and lower

leg can be mounted. The hip joint has 2 degrees of freedom: flexion-extension and vertical translation. The ankle joint can move medio-laterally and has all three rotational degrees of freedom. Thus, the rig provides the knee joint with all 6 degrees of freedom in order to reproduce its normal kinematics. Only the flexion angle of the knee is controlled directly. All other femorotibial translations and rotations are left free by the rig and are thus governed by the applied external forces and the geometry of the tested TKA design, as in a normal knee joint. Two motors are provided on the knee kinematics simulator. One motor moves the hip vertically, while a second motor applies load to a strap, which simulates the quadriceps tendon. Two constant force springs (50 N each) simulate the load of the medial and lateral hamstrings. Using the two motors, a weight-bearing squatting motion can be simulated with the knee. The first motor generates controlled flexion of the knee joint between 30° and 130° in 10 s, while the second motor simultaneously pulls the quadriceps tendon in such a way that a constant vertical force of 150 N is generated under the ankle. Sensors placed in line with the actuators detect the quadriceps and ankle forces and moments and hip height relative to the ankle.

Materials

As it is almost impossible to implant different total knee implants on cadaver specimens, metal bars were mounted on the knee rig to simulate femur and tibia for this project. Custom-made aluminum blocks were specially designed to accommodate femoral and tibial components of all tested implant designs. Collateral ligaments were simulated with rubber bands fixed to the aluminum blocks in the approximate location of the collateral ligaments insertion points. The patellar and quadriceps tendon were simulated with a single strap of woven nylon, distally fixed to the tibial tubercle and proximally to the motor simulating the quadriceps. The strap ran through a metal disk simulating the patella. The metal disk was designed in such a way that the patellar buttons of all tested implant designs could be cemented onto it. Medial and lateral hamstrings tendons were simulated with flexible metal cables, fixed to the anatomical position of their tibial insertion points on one side and to the constant force springs on the other end.

Eight contemporary PS TKA designs and one bicruciate-substituting design (BCS–TKA) were analyzed. All prostheses were left sided and medium size (Table 1). The femoral, tibial and patellar components of the investigated knee implants were cemented onto the custom-made metal blocks, according to the manufacturers' surgical technique guidelines to obtain correct alignment for all components in all designs with respect to tibial slope, femoral flexion and

rotation and patellar thickness and height. After implantation, the joint-line height and the Blackburne–Peel ratio were the same for all designs [4].

Data collection

For each investigated TKA design, five squats between 30° and 130° of flexion were performed on the knee simulator with a constant vertical ankle force of 150 N and medial and lateral hamstrings forces of 50 N each. A full squat was performed (flexion and extension phase), but only data from the flexion phase is reported here.

A pressure sensor (K-Scan 6900/10,000 psi, Tekscan® Inc., Massachusetts, USA) was covered with a 0.1-mm thin Teflon film to protect it against shear stresses and then calibrated in a loading frame (858 Mini Bionix II, MTS, Mn, USA) using 20 calibration points between 20 and 3,000 N. One sensor was then fixed to the posterior side and another to the anterior side of the inlay post using double- sided tape. During the squats, contact force, contact area and contact pressure between inlay post and the cam of the femoral component were simultaneously recorded with the K-Scan sensor at 20 Hz. The Tekscan sensor itself and also the protective PTFE cover and double-sided tape have different mechanical properties than the polyethylene and CoCr used in the implant components and may therefore lead to changes in contact pressures and areas. However, this is the only sensor available to measure contact mechanics dynamically. Tests and validations of the Tekscan system for this kind of application have been published [33, 34].

A 3D motion capture system was used (Vicon, Oxford, United Kingdom) to register knee kinematics during the squats at 100 Hz. Three infrared-reflective markers were fixed with double-sided tape on the upper leg and four on the lower leg. Four infrared-sensitive cameras with infrared-emitting strobe head units (MX40+, Vicon, Oxford, United Kingdom) were positioned around the knee allowing simultaneous recording of the markers trajectories in 3D. Before the test, the position of the markers with respect to anatomical landmarks was recorded to enable conversion of 3D marker trajectories to a meaningful description of knee kinematics afterward. The following landmarks were used: the centers of two circles fitted to the posterior medial and lateral femoral condyles, the center of the femoral component notch, the centers of two circles fitted to the tibial medial and lateral condyles, and the center of tibial component. The two longitudinal axes of the metal bars representing femur and tibia were considered as the anatomical axes of these two bones. Based on these anatomical features, coordinate

systems for femur and tibia could be defined, similar to the convention proposed by Grood and Suntay [10] and adapted by Victor et al. [29, 30].

Data analysis

After testing, the raw data from the Tekscan readings were synchronized with the Vicon kinematics data and the data obtained from the knee rig sensors (hip height and forces) during the squats. After synchronization, the raw Tekscan data were converted to contact force (in Newtons), contact area (in mm^2) and contact pressure (in MPa) based on Tekscan sensor calibration and then filtered using a low-pass Butterworth filter with order 10 and normalized cutoff frequency 0.04, to remove measurement noise. For each parameter, a mean curve was obtained from the five squat measurements. The 3D marker trajectories obtained from the Vicon measurements together with the positions of the markers with respect to the femoral and tibial coordinate systems were used to calculate tibiofemoral kinematics, as proposed by Grood and Suntay [10]. Thus, posterior femoral translation with respect to the tibia and tibial axial rotation could be derived. Femoral posterior motion was defined as the average of the posterior translation of the lateral and medial femoral condylar centers (FCC), projected on the transverse plane of the tibia. Tibial axial rotation was defined as the rate of change of the angle between the mediolateral axes of tibia and femur, both projected onto the transverse plane of the tibia. In both bones, the mediolateral axis is defined as the line joining the medial and lateral condyles centers.

The combination of pressure data from the Tekscan system and the tibiofemoral kinematics from the Vicon system enabled identification of the flexion angle, at which the post and cam mechanism engaged. The initial contact angle was simply defined as the first flexion angle when contact pressure was different from zero. Moreover, it also enabled presentation of the Tekscan data (contact pressure, contact area and contact force) as a function of flexion angle rather than time.

Statistical analysis

Previous tests showed that our technique is sufficiently accurate and precise to detect differences in translations (and lengths) and rotations of <2 mm and 2°, respectively [29].

Measurement accuracy of the Tekscan system is well documented in the literature, and it has been shown that it has an uncertainty of 6.5 % in resultant force, of 10.2 % for mean pressure and of 3.7 % for area [12, 33].

Repeating each squat five times checked reproducibility of the tests. However, no significance test for the differences between initial contact angles, contact forces, pressures or kinematics was performed as we considered the repeatability obtained with our setup as not representative for the conditions in which these different implants are used.

Correlations between contact mechanics parameters (force, pressure and area) and tibiofemoral kinematics were obtained using Excel 2003 (Microsoft Corporation, Redmond, Washington, USA).

Results

Results are shown in the combined plots per prosthesis (Figs. 2- 9).

Initial contact angle

Initial contact angle differs substantially from design to design and ranges between 43° for the Triathlon and 102° for the NexGen High-Flex. None of the designs showed loss of contact once a first contact was registered. Once the post and cam engage, they stay in contact until deepest flexion.

Contact force

All designs show a gradual increase in the contact force as function of the flexion angle. None of the designs showed anterior contact forces. A significant negative correlation, with a Pearson's correlation coefficient of -0.81, was found between maximal contact forces on the posterior tibial post and initial contact angle ($p = 0.009$). The Triathlon showed the highest maximal contact forces on the post in deep flexion, followed by the Journey, Genesis II HF, Vanguard, Scorpio NRG, NexGen HF, PFC Sigma and Scorpio.

Contact area

Contact area increases as a function of flexion angle. Designs with high forces on the post in deep flexion compensate with greater contact area. This is true for all designs except for the

Genesis II HF. The Journey has the biggest contact area in deep flexion, followed by the Triathlon, Scorpio, NexGen HF, Vanguard, Genesis II HF, Scorpio NRG and PFC Sigma.

Average and peak pressure

All designs show a gradual increase in average post-cam pressure as a function of flexion angle. The Genesis II HF design has the highest average pressure [above 25 MPa], followed by Triathlon, Vanguard, NexGen HF, Scorpio NRG, PFC Sigma, Journey and Scorpio.

The Scorpio NRG, Triathlon and Genesis II HF designs have the highest values in deep flexion (around 55 MPa), followed by Vanguard, NexGen HF, Journey, PFC Sigma and Scorpio. Maximum pressure increased as a function of flexion angle. For all designs, the local peak pressure exceeded the yield stress of around 22 MPa for UHMWPE [15].

In Figs. 2- 9, on the right side, a pressure map indicating the peak pressure in every location on the post as well as the trajectory of the center of pressure is shown. Below this, the peak pressure over the entire region as a function of flexion angle is shown.

Height of the center of pressure and bending moment

The height of the centre of pressure (COP) was defined as the distance from the COP to the deepest point of the tibial polyethylene, as a function of flexion angle. It decreased with increasing flexion angle except for the Scorpio and PFC Sigma. The bending moment on the post was calculated over the entire range of flexion. A gradual increase in moment toward deep flexion was found, except for the Triathlon, for which the moment increased until 110°, and then decreased in deeper flexion. Highest values of moments were found for the Triathlon followed by the Journey, Vanguard, PFC Sigma, NexGen HF, Genesis II HF, Scorpio and Scorpio NRG.

Kinematics: femoral posterior motion and tibial rotation

In Figs. 2-9, on the left side, a top view is shown of the tibial insert, indicating the projections of the lateral and medial FCC in 40° of flexion and in 130° of flexion. The posterior translation of both FCC is plotted as a function of flexion angle.

The lateral femoral posterior motion after contact, defined as the total posterior translation of the lateral condyle after the cam engages with the post, ranges from 5.6 mm for the Scorpio to 15.4 mm for the Triathlon. (Table 2).

The tibial rotation after contact, defined as the largest internal or external rotation measured during flexion after the cam engages with the post, shows a large variability. Rotations ranged from 2.1 ° for Vanguard to 8.7 ° for Journey (Table 2).

Discussion

The most important finding of the present study was the finding of a correlation of lateral femoral posterior motion with tibial rotation after post-cam contact with maximum contact forces (multiple correlation coefficient of 0.77). This suggests that designs with more natural femoral posterior motion have higher contact forces. Due to the earlier engagement and stronger post guidance a more physiologic motion exists. This assumption is confirmed with a good correlation between initial contact angles and maximal contact forces, and thus between the initial contact angle and femoral posterior motion. This confirms the findings of Chandran et al. [6] that the post-cam design determines the amount of posterior femoral motion and guides the motion in the designs, especially in high flexion [15]. Designs with early engagement are the Triathlon, Journey, Genesis II HF, Vanguard and Scorpio designs, with engagement before 80° of flexion. The NexGen HF designs engage after 100° of flexion, resulting in less guidance of motion. Toutoungi et al. found that the PCL is functional after 50° of flexion. This makes us believe that the ideal initial contact angle should be around 50° of flexion for PS designs [24].

PS TKA has been introduced as an alternative for CR designs when the PCL is missing or a-functional and to obtain more natural kinematics. PS designs rely on their post-cam mechanism to obtain posterior motion of the femur. Kinematics is thought to be more natural although this is controversial and at least implant dependent [3, 23]. Post-cam mechanism should stabilize the knee in flexion [24], should increase the quadriceps muscle efficiency, should improve flexion and should reduce the shear forces on the tibia [14]. Post-cam failures are described such as breakage, dislocations and failure of the guided motion [2, 8, 12, 15, 20]. Transmission of these high stresses to the modular and bone–implant interfaces potentially leads to backside wear or loosening [5, 18, 19, 26]. However, good clinical results are seen, without catastrophic failures in vivo.

All designs showed post-cam pressures exceeding the yield stress of UHMWPE (~22 MPa), suggesting other important features to explain the absence of catastrophic failure, such as differences in bending height and height of peak pressure on the post. These values fairly match the result of Fitzpatrick et al. in their study about post-cam mechanics [5, 18, 19, 26].

Designs with higher contact forces compensate for these higher forces with a larger contact area, in order to reduce their contact pressure and avoid post failure [14]. This is true for all prosthetic designs except for the Genesis II, which has a relative small contact area and high contact forces. Despite this, no catastrophic failures are seen clinically for this design, and it has excellent long-term results without post breakage. A possible explanation for this finding is the relatively low moment on the post that possibly compensates for the high pressures. All designs except the Scorpio and the PFC Sigma had a gradual decrease in their center of force on the tibial post during flexion. This confirms what Argenson et al. [1] found and contributes to the stability of the system in flexion with lower jump distances from the post relative to the cam [2, 15, 20].

One limitation of this study is the strict in vitro setting with absence of knee capsule and ligaments and the fact that the knee rig was not validated for prostheses mounted on metal fixtures. However, our kinematic measurements for the Journey design are close to the kinematics measured in cadaveric knees implanted with a Journey and tested in the same setup [24]. The initial contact angle for the Journey prosthesis matches with previous data from knee simulations and in vivo testing [11, 28]. Our amount of lateral femoral posterior motion between 30° and 130° flexion matches fairly with the results of Johal et al. in their MRI study in the native knee [11]. Shimizu et al. measured the kinematics of the NexGen LPS-Flex design during an in vivo squat with fluoroscopy [21]. Their results closely match our results for NexGen LPS-Flex: post-cam engagement at 93.4° (vs. 102° in this study), lateral femoral posterior motion after contact of 5.1 mm (vs. 5.9 mm in this study), negligible femoral rotation after contact. The location of the contact area is similar. Despite these limitations, testing conditions were the same for all prostheses, and thus, a comparison between different designs is certainly possible. The absence of soft tissues guarantees a strict comparable setting for all designs.

A strong point is the correlation with knee kinematics, since there are, to our knowledge, only two previous study available that correlate the post-cam contact mechanics with knee kinematics during a squat movement [13]. Our results regarding femoral posterior motion of the NexGen LPS prosthesis in a cadaver model with static measurement of post-cam stresses

are very similar. However, the maximum post-cam forces were considerably lower, and the initial contact angle was about 90°, which is earlier than in our results. This difference could be explained by the different testing conditions of both studies: NexGen LPS versus NexGen LPS-Flex, difference in quadriceps load and hamstrings force, etc.

Comparing all prosthetic kinematics to normal knee motion, we can conclude that none of the existing PS TKA designs can produce normal knee kinematics in terms of posterior femoral translation, tibial rotation and PCL forces [22, 24, 25]. The Journey prosthesis remains closest to normal native knee kinematics, but gives rise to new problems as over steering and lateral knee pain and post-cam dislocation [2, 17]. On the other hand, with this design lots of people claim a 'forgotten knee' after implantation. This makes us believe that normal knee kinematics is the key in improving our existing total knee designs. Most of the designs show an a-functional post-cam design, which is not able to act as a PCL does in the natural knee. Maybe, this is one of the reasons that in the past no difference in clinical outcome was found between PS and CR knees.

Conclusion

Total knee contact mechanics is documented in a standardized manner in eight contemporary total knee designs during dynamic knee testing. A strong correlation was found between lateral femoral rollback and maximum contact forces. No design showed ideal kinematics. In all designs, high peak stresses were found. Designs with higher guidance of the post-cam system showed higher stresses and thus higher risk for failure. Further investigation of the post-cam mechanics has to be done, and more functional post-cam designs need to be developed.

References

1. Argenson Jn, Scuderi GR, Komistek RD et al (2005) In vivo kinematic evaluation and design considerations related to high flexion in total knee arthroplasty. J Biomech 38(2):277–284
2. Arnout n, Vandenneucker H, Bellemans J (2011) Posterior dislocation in TKR, a price for deep flexion? Knee Surg Sports Traumatol Arthrosc 19(6):911–913
3. Banks SA, Markovich GD, Hodge WA (1997) In vivo kinematics of cruciate-retaining and substituting knee arthroplasties. J Arthroplasty 12(3):297–304
4. Blackburne JS, Peel Te (1977) A new method of measuring patellar height. J Bone Joint Surg Br 59-B:241–242
5. Callaghan JJ, O'Rourke MR, Goetz DD et al (2002) Tibial post impingement in posterior stabilized total knee arthroplasty. CORR 404:83–88

6. Chandran n, Amirouche F, Gonzalez MH et al (2003) Optimization of the posterior stabilized tibial post for greater femoral roll back after TKA, a finite element analysis. Int Orthop 33(3):687–693
7. Christen B, Heesterbeek P, Wymymga A, Wehrli U (2007) Posterior cruciate ligament balancing in total knee replacement: the quantitative relationship between tightness of the flexion gap and tibial translation. JBJS Br 89(8):1046–1050
8. Clarke HD, Math KR, Scuderi GR (2004) Polyethylene post failure in posterior stabilized total knee arthroplasty. J Arthroplasty 19(5):652–657
9. Fitzpatrick CK, Clary CW, Cyr AJ et al (2013) Mechanics of post-cam engagement during simulated dynamic activity. J Orthop Res 31(9):1438–1446
10. Grood eS, Suntay WJ (1983) A joint coordinate system for the clinical description of three-dimensional motions: application to the knee. J Biomech eng 105:136–144
11. Hamai S, Miura H, Matsuda S et al (2010) Contact stresses at the anterior aspect of the tibial post in posterior-stabilized total knee replacement. JBJS 92-A:1765–1773
12. Harris ML, Morberg P, Bruce WJM, Walsh WR (1999) An improved method for measuring tibiofemoral contact areas in total knee arthroplasty: a comparison of K-scan sensor and Fuji film. J Biomech 32(9):951–958
13. Johal P, Williams A, Wragg P, Hunt D, Gedroyc W (2005) Tibiofemoral movement in the living knee. A study of weight bearing and non-weight-bearing knee kinematics using 'interventional' MRI. J Biomech 38(2):269–276
14. Jung KA, Lee SC, Hwang SH, Kim SM (2009) Fractured polyethylene tibial post in a posterior-stabilized knee prosthesis presenting as a floating palpable mass. J Knee Surg 22(4):374–376
15. Li G, Most e, Otterberg e et al (2002) Biomechanics of posterior- substituting total knee arthroplasty: an in vitro study. Clin Orthop Relat Res 404:214–225
16. Li G, Zayontz S, Most e et al (2001) Cruciate retaining and cruciate substituting total knee arthroplasty. An in vitro comparison of the kinematics under muscle loads. J Arthropl 16(8 Suppl 1):150–156
17. Lombardi AV, Mallory TH, Vaughn BK et al (1993) Dislocation following primary posterior-stabilized total knee arthroplasty. J Arthroplasty 8:633–639
18. Luyckx L, Luyckx T, Bellemans J, Victor J (2010) Iliotibial band traction syndrome in guided motion TKA: a new clinical entity in TKA. Acta Orthop Belg 76(4):507–512
19. nakayama K, Matsuda S, Miura H et al (2005) Contact stress at the post cam mechanism in posterior stabilized total knee arthroplasty. JBJS Br 87(4):483–488
20. O'Rourke MR, Callaghan JJ, Goetz DD et al (2002) Osteolysis associated with a cemented modular posterior cruciate substituting total knee design: five to eight -year follow-up. JBJS 84:1362–1371
21. Puloski SK, Mc Calden RW, Mac Donald SJ et al (2001) Tibial post wear in posterior stabilized total knee arthroplasty. An unrecognized source of polyethylene debris. JBJS 83:390–397
22. Sharkey PF, Hozack WJ, Booth Re et al (1992) Posterior dislocation of total knee arthroplasty. Clin Orhop Rel Res 278:128–133

23. Shimizu n, Tomita T, Yamazaki T et al (2011) The effect of weight-bearing condition on kinematics in a high flexion, posterior stabilized total knee design. J Arthroplasty 26(7):1031–1037
24. Stiehl JB, Komistek RD, Dennis DA et al (1995) Fluoroscopic analysis of kinematics after posterior cruciate retaining knee arthroplasty. J Bone Joint Surg Br 77(6):884–889
25. Toutoungi De, Lu TW, Leardini A et al (2000) Cruciate ligament forces in the human knee during rehabilitation exercises. Clin Biomech 15(3):176–187
26. van Duren BH, Pandit H, Price M et al (2012) Bicruciate substituting total knee replacement: how effective are the added kinematic constraints in vivo? Knee Surg Sports Traumatol Arthrosc 20(10):2002–2010
27. Verra WC, van den Boom LG, Jacobs W, Clement DJ, Wymenga AA, nelissen RG (2013) Retention versus sacrifice of the posterior cruciate ligament in total knee replacement for treatment of osteoarthritis and rheumatoid arthritis, Cochrane review
28. Victor J, Kyle JP, Mueller BS et al (2010) In vivo kinematics after a cruciate-substituting TKA. CORR 468:807–814
29. Victor J, Vanglabbeek F, Vander Sloten J, Parizel PM, Somville J, Bellemans J (2009) An experimental model for kinematic analysis of the knee. J Bone Joint Surg Am 91:150–163
30. Victor J, Van Doninck D, Labey L, Innocnti B, Parizel PM, Bellemans J (2009) How precise can bony landmarks be determined on a CT scan of the knee. Knee 16(5):358–365
31. Wasielewski RC (2002) The causes of insert backside wear in total knee arthroplasty. CORR 404:232–246
32. Waslewski GL, Marson BM, Benjamin JB (1998) early incapacitating instability of posterior cruciate ligament-retaining in total knee arthroplasty. J Arthroplasty 13(7):763–767
33. Wilson DR, Apreleva MV, eichler MJ, Harrold FR (2003) Accuracy and repeatability of a pressure measurement system in the patellofemoral joint. J Biomech 36(12):1909–1915
34. Wirz D, Becker R, Li SF, Friederich nF, Müller W (2002) Validation of the Tekscan system for statistic and dynamic pressure measurements of the human femorotibial joint. Biomed Tech (Berl) 47(7–8):195–201

Table 1: List of the TKA designs used in this study with their sizes

Design	Implant name	Size femur	Size tibia	Size patella
1	Genesis II high-flex	5	5	32
2	Journey BCS I	6	6	32
3	NexGen LPS-flex	E	CD	32
4	PFC sigma	3	4	
5	Scorpio high-flex	7	7	7
6	Scorpio NRG	6	7	7
7	Triathlon	4	4	A35
8	Vanguard	62.5	71/75	31

Genesis II high-flex and Journey BCS I are registered trademarks of Smith and Nephew; NexGen LPS-flex is a registered trademark of Zimmer. PFC Sigma is a registered trademark of DePuy, Johnson & Johnson. Scorpio High-Flex, Scorpio NRG, Triathlon are registered trademarks of Stryker Howmedica. Vanguard is a registered trademark of Biomet

Table 2: Average values and SDs (between brackets) for maximal post-cam contact force, initial contact angle, lateral femoral posterior motion after contact and femoral rotation after contact are given

Design	Max. contact force (N)	Initial contact angle (deg)	Lateral femoral posterior motion after contact (mm)	Femoral rotation after contact (deg)
Scorpio	318 (78.6)	79 (3.0)	5.6 (1.5)	3.1 (1.2)
PFC sigma	394 (19. 5)	89 (2.4)	10 (0.4)	4 (0.2)
NexGen HF	443 (12.5)	102 (0.3)	5.9 (0.3)	1.4 (0.2)
Scorpio NRG	518 (25.8)	80 (1.6)	13.8 (1.2)	2.8 (0.4)
Vanguard	771 (36.3)	76 (2.5)	11.6 (0.2)	2.1 (0.4)
Genesis II HF	820 (41.3)	71 (4.0)	11.3 (0.1)	8.3 (0.4)
Journey BCS I	888 (41.5)	56 (3.9)	9.7 (0.3)	8.7 (1.5)
Triathlon	962 (43.6)	43 (10.1)	15.4 (0.6)	3.7 (0.9)

Listed according to increasing contact force

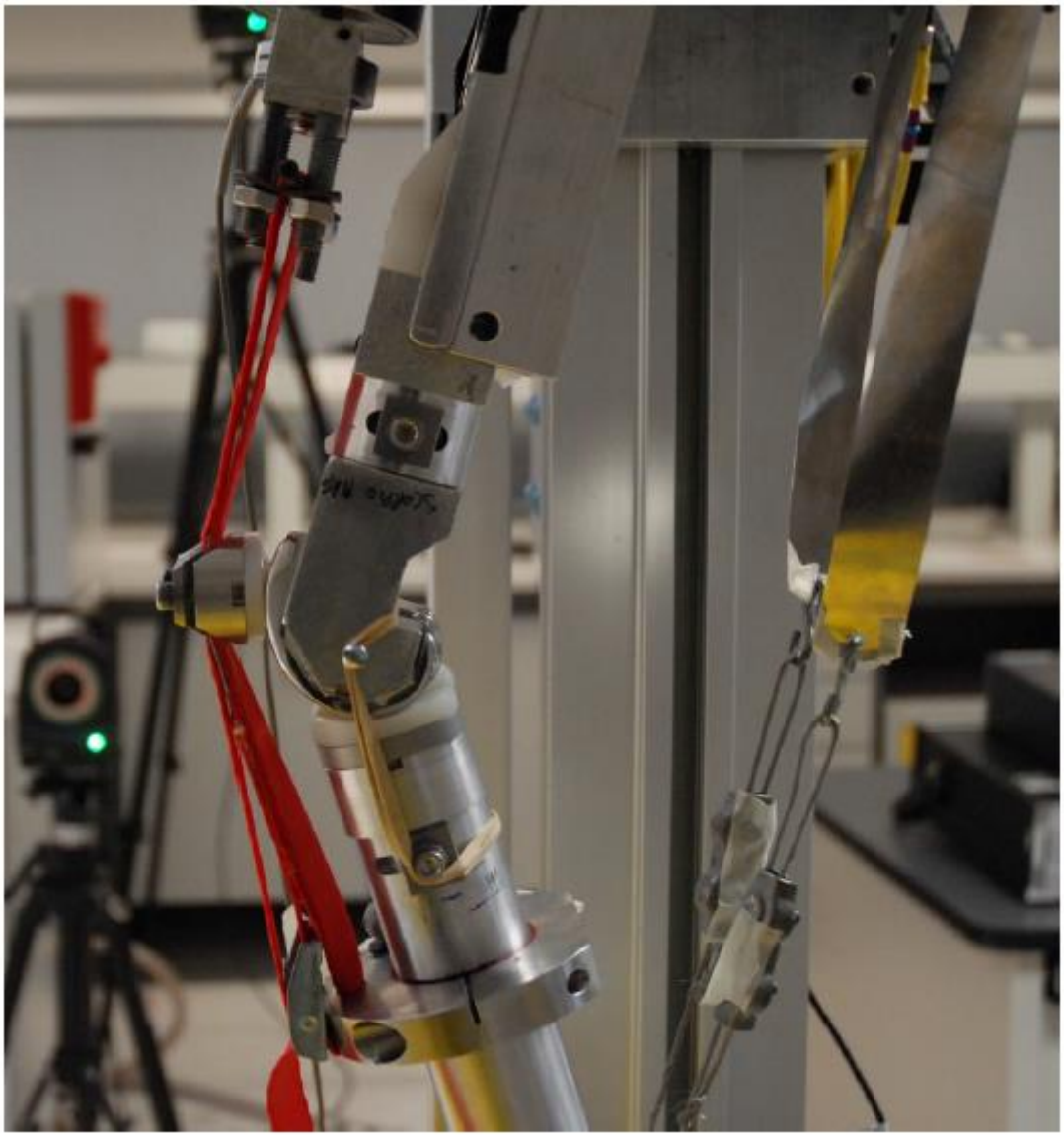

Fig. 1 Test set-up

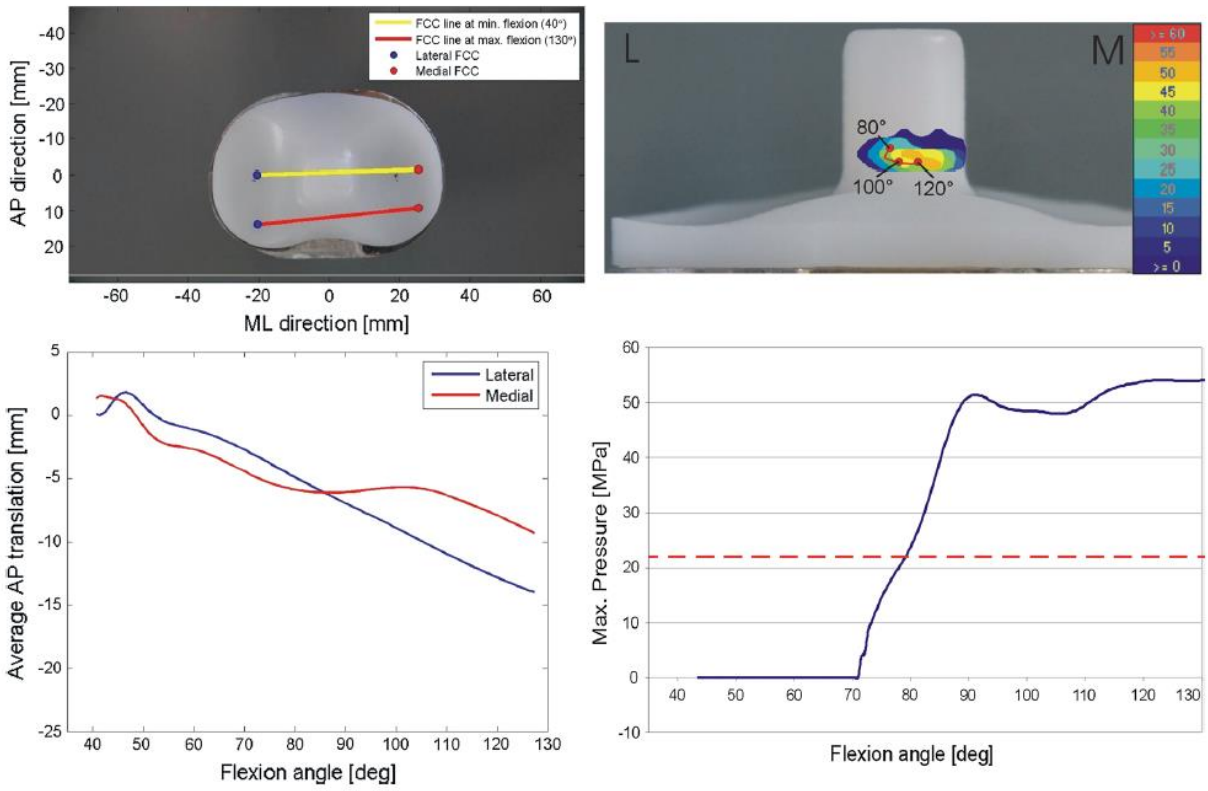

Fig. 2 Genesis

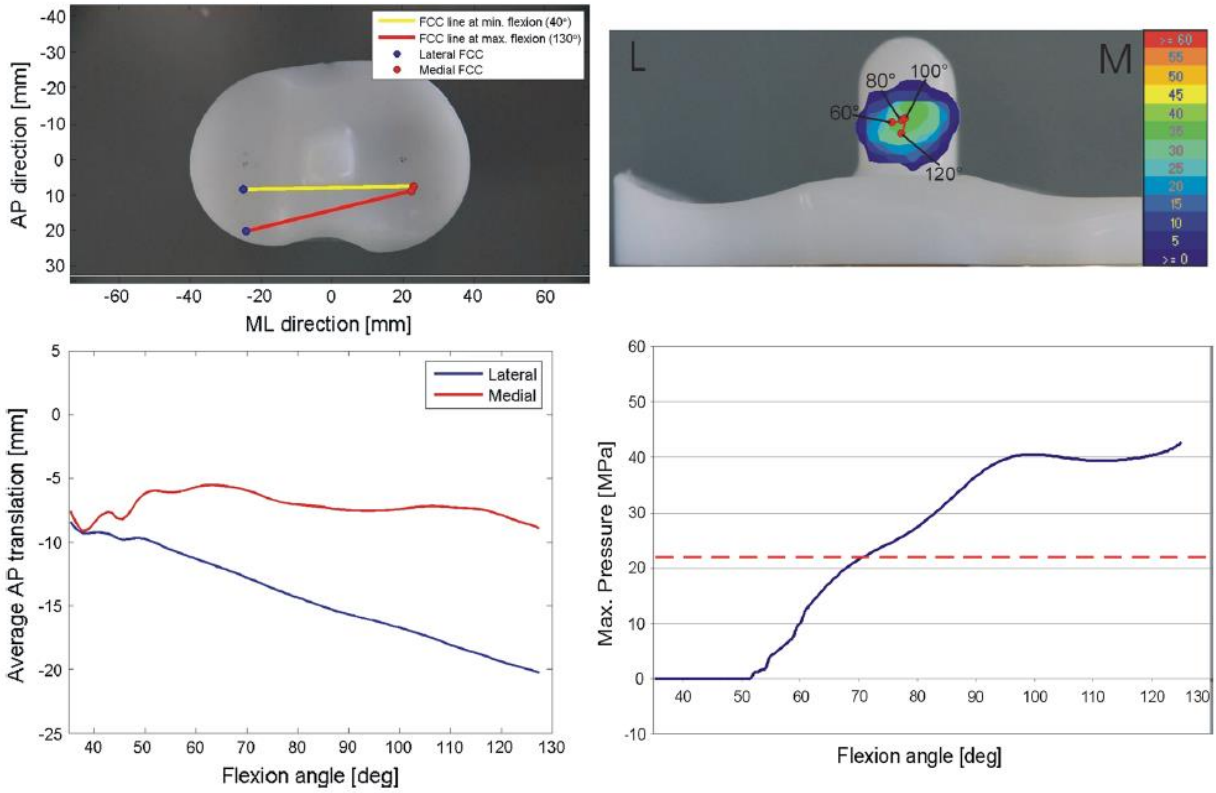

Fig. 3 Journey

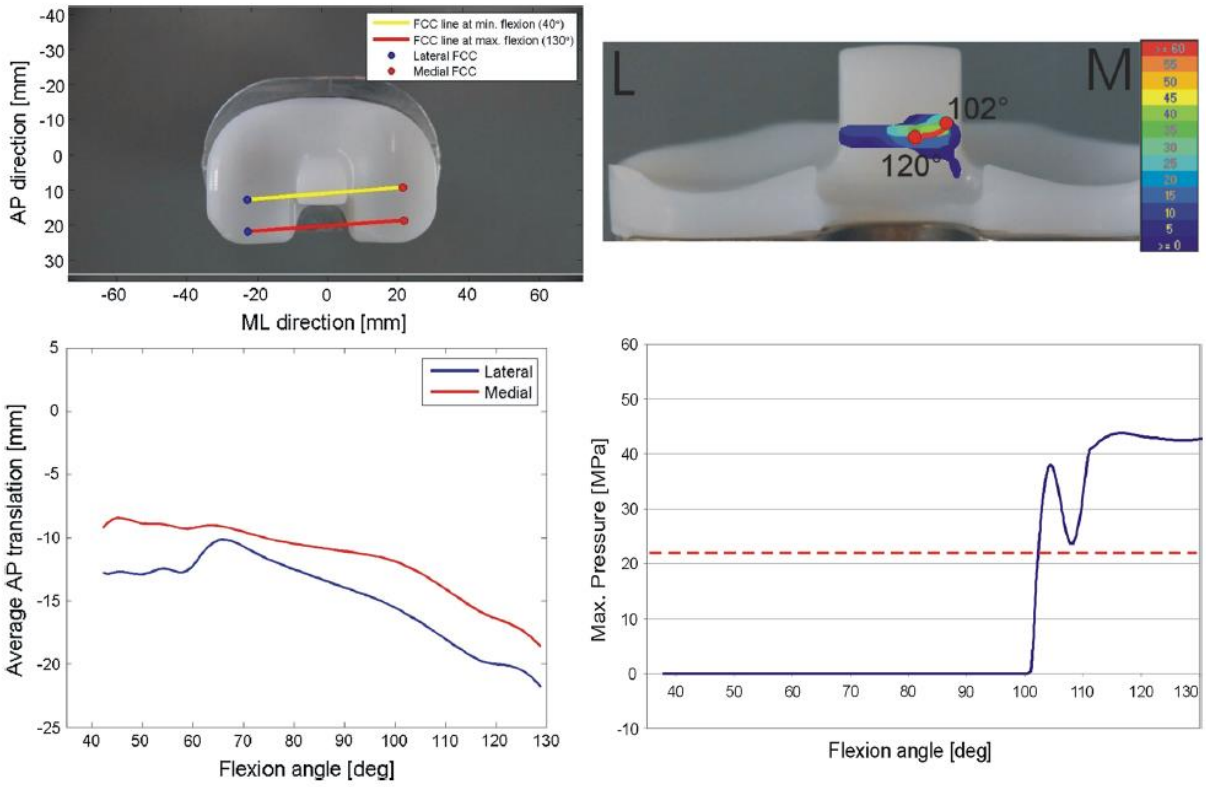

Fig. 4 NexGen

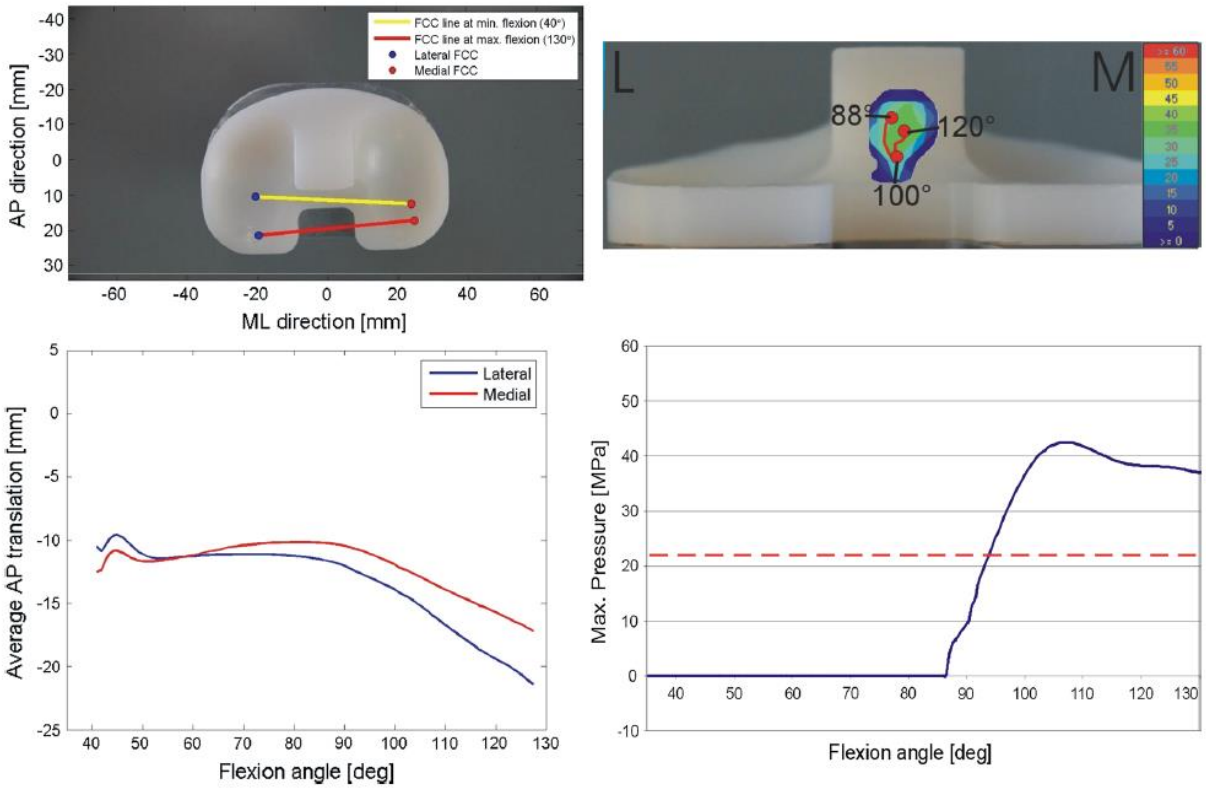

Fig. 5 PFC Sigma

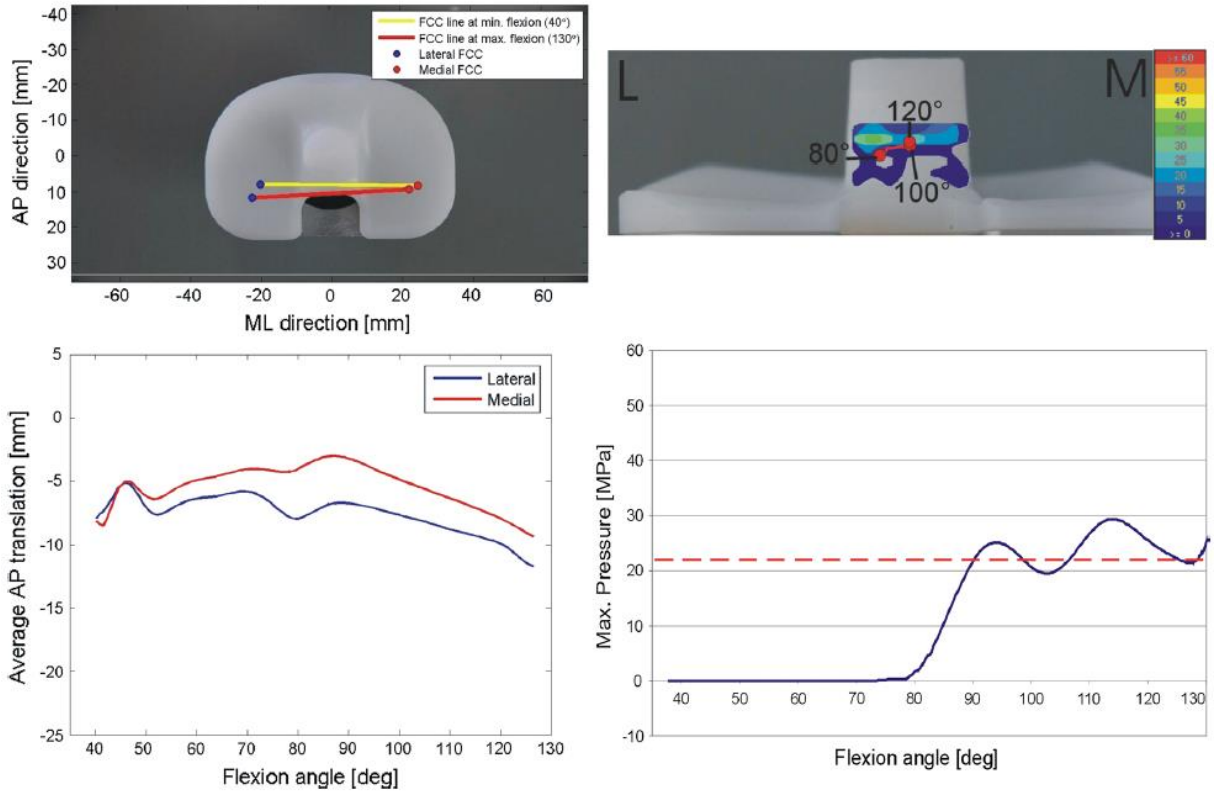

Fig. 6 Scorpio

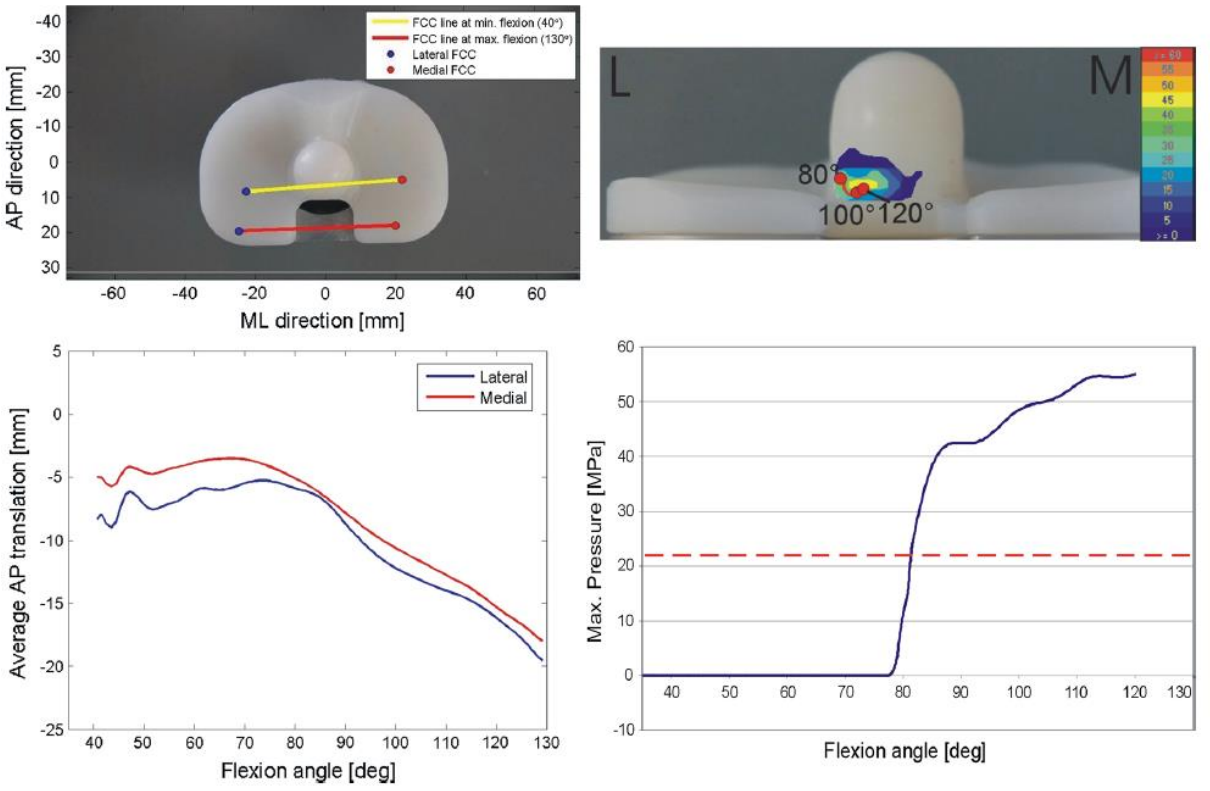

Fig. 7 Scorpio NRG

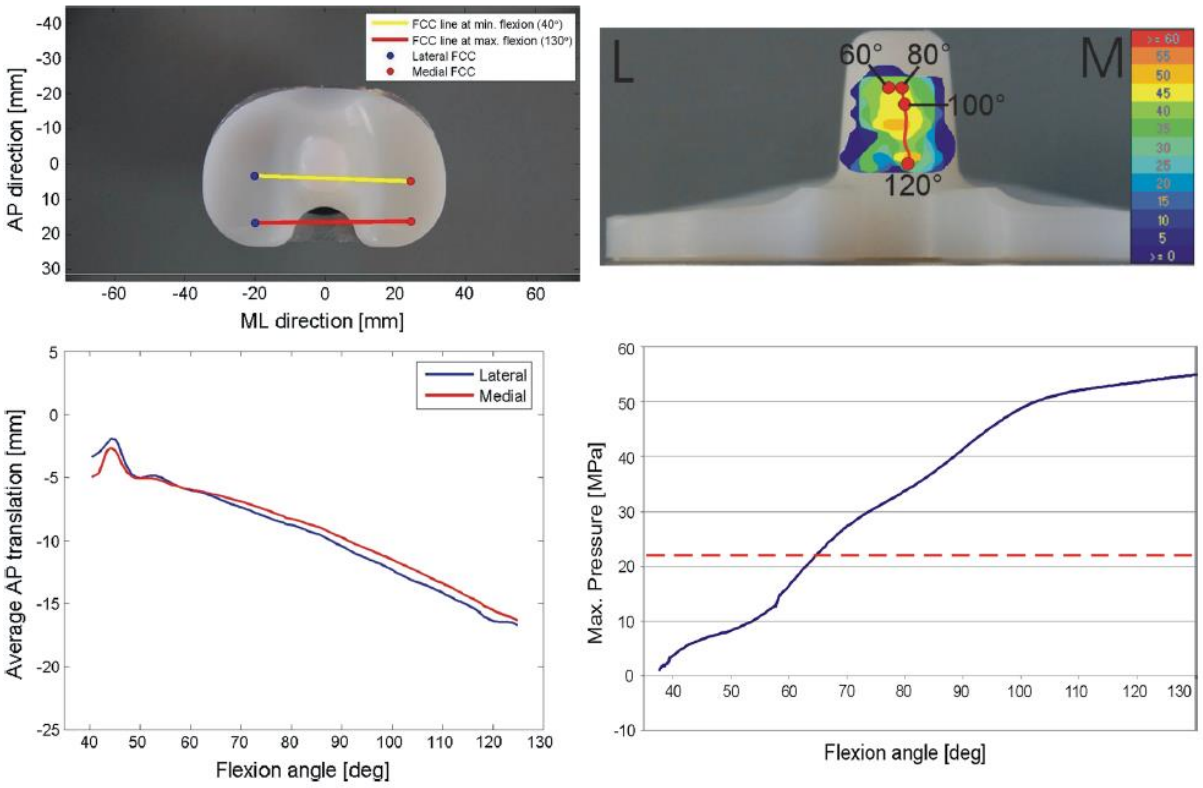

Fig. 8 Triathlon

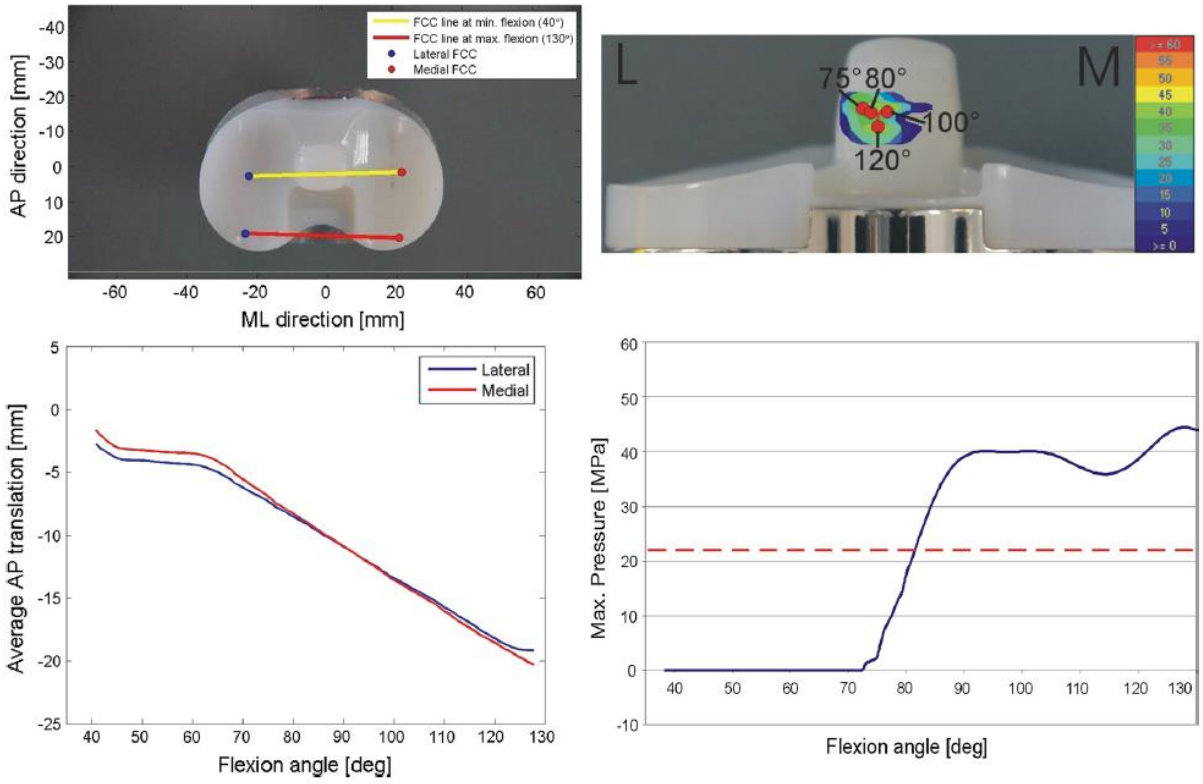

Fig. 9 Vanguard